



HAL
open science

How soft substrates affect the buckling delamination of thin films through crack front sink-in

R. Boijoux, G. Parry, J.-Y. Faou, C. Coupeau

► **To cite this version:**

R. Boijoux, G. Parry, J.-Y. Faou, C. Coupeau. How soft substrates affect the buckling delamination of thin films through crack front sink-in. *Applied Physics Letters*, 2017, 110 (14), 10.1063/1.4979614 . hal-01685184

HAL Id: hal-01685184

<https://hal.science/hal-01685184>

Submitted on 9 Apr 2024

HAL is a multi-disciplinary open access archive for the deposit and dissemination of scientific research documents, whether they are published or not. The documents may come from teaching and research institutions in France or abroad, or from public or private research centers.

L'archive ouverte pluridisciplinaire **HAL**, est destinée au dépôt et à la diffusion de documents scientifiques de niveau recherche, publiés ou non, émanant des établissements d'enseignement et de recherche français ou étrangers, des laboratoires publics ou privés.

How soft substrates affect the buckling delamination of thin films through crack front sink-in

R. Boijoux, G. Parry, J.-Y. Faou, and C. Coupeau

Citation: *Appl. Phys. Lett.* **110**, 141602 (2017); doi: 10.1063/1.4979614

View online: <http://dx.doi.org/10.1063/1.4979614>

View Table of Contents: <http://aip.scitation.org/toc/apl/110/14>

Published by the [American Institute of Physics](#)

Fearful for the future of science?

Programs and Resources | Publications | Career Resources | Member Societies | About AIP | [Contact Us](#)

FYI
AMERICAN INSTITUTE OF PHYSICS

on authoritative news and resources

FYI This Week
A newsletter, issued each Monday evening and covers the upcoming week and its features for physics.

The Week Ahead
A weekly app for mobile devices (iOS and Android) that provides a quick overview of the week's events.

Plus: Career Opportunities

Sign up for FREE FYI emails.
AIP | American Institute of Physics

FYI Bulletin

How soft substrates affect the buckling delamination of thin films through crack front sink-in

R. Boijoux,^{1,2,a)} G. Parry,¹ J.-Y. Faou,³ and C. Coupeau²

¹University Grenoble Alpes, SIMaP, 38000 Grenoble, France

²University Poitiers, Institut P², 86962 FUTUROSCOPE, Chasseneuil, France

³Saint-Gobain Research, 93303 Aubervilliers, France

(Received 24 January 2017; accepted 21 March 2017; published online 3 April 2017)

As the development of stretchable devices advances, engineering components with rigid films on soft substrates are becoming more numerous. We propose to analyse the buckle delamination of a film on a soft substrate, under a biaxial compressive stress state. This problem has already been investigated by an Euler column buckling analysis. In this paper, experiments on soft substrates are presented, which demonstrate that the buckle shape is, in some cases, better approximated by a “Mexican hat” shape. A model using a non-linear plate bonded to an elastic medium by a cohesive interaction is used to describe the delamination process. It is demonstrated that the “Mexican hat” shape modifies the crack propagation behavior for a soft substrate. *Published by AIP Publishing.*
[\[http://dx.doi.org/10.1063/1.4979614\]](http://dx.doi.org/10.1063/1.4979614)

Thin films and coatings are widely used in several scientific fields, for instance, in mechanics or microelectronics. High internal stresses are often observed, typically about a few GPa, in compression when the films or coatings are prepared through physical vapor deposition. The films are then susceptible to delaminating and buckling, resulting in interesting but complex structures at the free surfaces of the materials.^{1–4} The buckling phenomenon has been extensively studied in the past few decades since it generally leads to the loss of functional properties provided by the film/substrate systems. A mapping of stable morphologies has been previously established from finite element simulations.⁵ It explains the appearance of the most common buckling structures, i.e., the straight-sided, the circular, and the telephone cords. The buckling behavior has also been analytically characterized in the framework of the Föppl–von Kármán theory of thin plates.^{6,7} In the simple case of a rigid substrate and of a 1D straight-sided buckle, a critical stress for buckling to occur has been determined and is associated with a sinusoidal profile of the equilibrium shape.⁸ Moreover, the effect of the elasticity of the substrate has been studied by finite element simulations. It is shown that the critical stress for buckling is significantly reduced when the soft character of the substrate is increased, while the maximum deflection is increased.⁹ In particular, it was demonstrated that the sinusoidal equilibrium shape is no longer valid. Instead, small depressions are present, at the nanometer scale, on both sides of the 1D buckle,^{9–11} which will be referred to as a “Mexican hat” shape hereafter.

It is now well established that the mixed mode loading on the crack front is of primary importance for the buckle propagation mechanism. An increase in the mode II contribution (shear traction) compared to the mode I (normal traction) generally increases the effective toughness of the interface.^{8,12–16} The dependence of the elastic mismatch of

the film/substrate system on mode mixity has also been analytically highlighted. However, these analytical developments were performed assuming a sinusoidal shape for the buckle equilibrium shape, even for soft substrates. In this context, we present a study of the influence of the “Mexican hat” shape on the buckling delamination of rigid films on soft substrates. Atomic force microscopy investigations of buckles are first presented. Finite element simulations are then described and compared to the analytical solutions available in the literature.

Ni and Au thin films were deposited by physical vapor deposition on polycarbonate substrates (PC) and Si wafers, respectively. The thickness ratio of these systems is $H_{PC}/h_{Ni} = 10^4$ and $H_{Si}/h_{Au} = 1500$, with H and h being the substrate and film thicknesses, respectively ($H_{PC} = 2$ mm, $H_{Si} = 600$ μ m, $h_{Ni} = 200$ nm, and $h_{Au} = 400$ nm). The properties of each film/substrate system is characterized by its Dundurs coefficient, $\alpha_{Ni/PC} = 0.97$ and $\alpha_{Au/Si} = -0.17$, respectively. The coefficient is given by $\alpha = (\overline{E}_f - \overline{E}_s) / (\overline{E}_f + \overline{E}_s)$, with $\overline{E}_i = E_i / (1 - \nu_i^2)$ being the reduced modulus of the film or of the substrate. The reduced modulus ranges from -1 (hard substrate) to $+1$ (soft substrate). The PC substrates were then deformed under uni-axial compression at room temperature and atmospheric conditions. As expected,^{9,17} 1D straight-sided buckles are generated with an orientation perpendicular to the compression axis, as observed in Fig. 1(a). For the Au/Si systems, buckling was induced by putting the coated materials in water for a few seconds, which alters the adhesion properties. In Fig. 1(b), the profile of a characteristic 1D buckle for the two systems, measured by atomic force microscopy images, is presented. First, it is shown that for $\alpha_{Au/Si} = -0.17$, the equilibrium profile stays close to the sinusoidal shape expected for a stiff substrate, i.e., for $\alpha = -1$. For $\alpha_{Ni/PC} = 0.97$, the sinusoidal shape is no longer valid. The equilibrium profile is now characterized by small depressions of only a few nanometers in depth at both sides of the buckle ($x/b = \pm 1.5$ in Fig. 1(b)). These investigations were performed under external loading to induce a straight-sided

^{a)}Author to whom correspondence should be addressed. Electronic mail: romain.boijoux@simap.grenoble-inp.fr

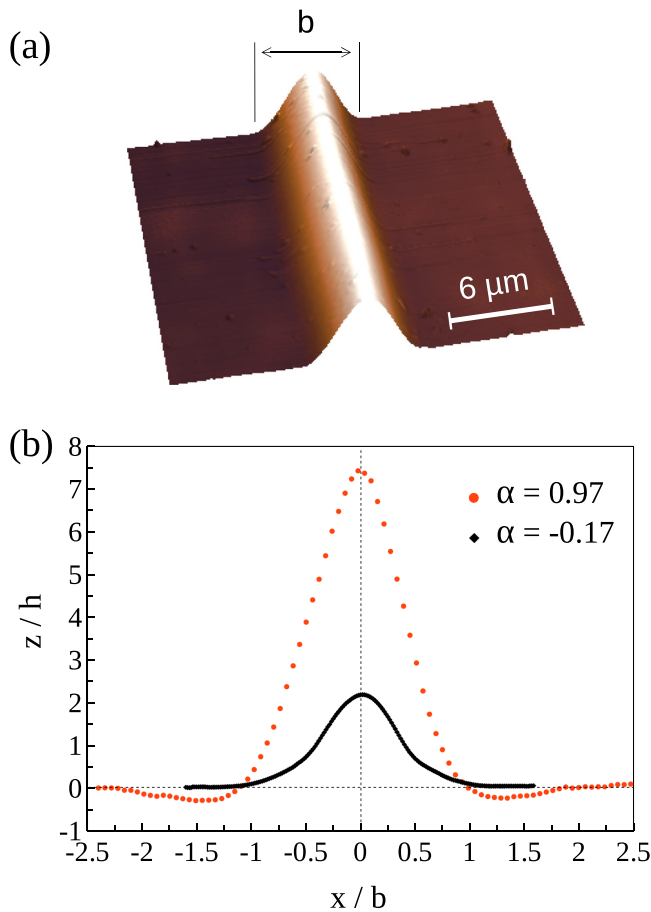


FIG. 1. Sink-in effect at the buckle edges induced by the substrate compliance. (a) AFM topography image of a straight sided buckle and (b) Euler column profile ($x = -0.17$) and its “Mexican hat” counterpart ($x = 0.97$).

buckle.⁵ It is however believed that there is no influence of the type of loadings applied for the depressions to be present. As previously reported,⁹ the depressions occur as the stiff film wedges sink into the soft substrate close to the crack front, in an area where the film is still bonded to the substrate. This so-called “Mexican hat” profile is remarkably different from the one predicted by the classical unilateral buckling solution (the Euler column). Thus, it is likely that an analysis based on the real shape of the buckle may lead to different predictions regarding the crack propagation at the film/substrate interface, at least for values of Dundur’s coefficient, α , close to 1.

To study the buckle delamination, we use a mechanical model consisting of three regions depicted in Fig. 2. The thin film is modeled as a geometrically non-linear plate. The mid-plane surface is defined by the (O, x, y) plane, with (u, v, w) the respective displacement components along the (Ox, Oy, Oz) axes for any point of the mid-plane. The substrate is represented by a bulk three-dimensional region.

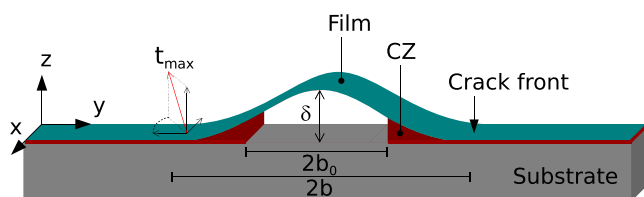


FIG. 2. Schematic FEM representation.

Both materials of the film and the substrate are considered as linear elastic isotropic. A thickness ratio of $H/h = 100$ between the film and the substrate is used. It should be emphasized that the substrate may be plastically deformed during the buckling process, especially near the “Mexican hat”. This may lead to marks or imprints at the interface.¹⁸ To incorporate such plastic events, it would be necessary to implement a plastic law in the FEM code, which is beyond the scope of this paper.

For the interface debonding process, a mixed-mode cohesive zone (CZ) model is used. Cohesive zone models have been widely used in fracture mechanics over the past two decades.^{19–23} The constitutive behavior of the interface consists of a traction-separation law. Due to the interaction between the two separating faces, the interface traction \bar{T} depends on the separation vector $\bar{\delta}$, which is the relative displacement between opposite crack faces at a point initially joined on the interface. The separation and traction vectors can be resolved into their normal components (δ_n, T_n) , the opening or mode I contribution, and into their tangential components resolved in the direction normal to the crack front, (δ_t, T_t) , the shearing or mode II contribution.

Finally, to account for large values of the out-of-plane displacement $w(x, y)$, the calculation must be carried out within the framework of large displacements using the Green-Lagrange strain tensor. The loading consists of an eigenstrain $\epsilon_0 > 0$ applied uniformly to the plate ($\epsilon_{xx} = \epsilon_{yy} = \epsilon_0$, $\epsilon_{xy} = 0$) at time $t = 0$, resulting in an equi-biaxial compressive stress state generated in the flat adherent parts of the film: $\sigma_{xx} = \sigma_{yy} = -E_f \epsilon_0 / (1 - \nu_f) = -\sigma_0$, $\sigma_{xy} = 0$. A delaminated zone of the film of width $2b_0$ (area with no adhesion) is initially introduced. The length b_0 was chosen based on the minimal length necessary to make the film buckle at the given stress level, σ_0 . Symmetric boundary conditions are assumed at the domain limits along the x direction. The bottom of the substrate is prevented from moving in the z direction. The numerical integration of the model is carried out using the finite elements software ABAQUS with an explicit quasi-static procedure.

The standard cohesive element (COH) from the ABAQUS library was used to model the cohesive zone (located everywhere along the interface), with a linear/softening model for the traction separation behavior (see, e.g., Faou *et al.*²⁴ for a complete description). One important feature of the cohesive model we are using is that the separation energy/area, $G_c(\psi)$, has a dependence on mode mixity characterized by a phenomenological relation given by^{8,25}

$$G_c(\psi) = G_{Ic} (1 + \tan^2(\eta\psi)). \quad (1)$$

In this expression, G_{Ic} is the mode I separation energy or toughness. ψ is the mode mixity parameter measuring the mode II to mode I loading at the interface, which will be further discussed in the following. Finally, η is the parameter controlling the mode mixity’s dependence on interface toughness. The values of η close to zero imply a weak dependence on the mode mixity, while the values close to unity have a strong dependence. In our case, we take $\eta = 0.9$, as in the Hutchinson and Suo model.⁸

At this point, it is worth emphasizing a fundamental difference between the cohesive zone models and the model of classical linear elastic fracture mechanics (LEFM). In the cohesive law, the measure of the mode mixity ψ is defined in terms of the combination of tractions at the interface, as $\tan(\psi) = T_t/T_n$. This definition differs from that employed in linear fracture mechanics because it is defined point-wise on the interface in the vicinity of the crack front (i.e., from element to element). In contrast, the conventional definition of mode mixity ψ in LEFM is defined in terms of the mode I and mode II stress contributions at the crack front. More precisely, for an interface crack between two dissimilar materials, the oscillatory singularity of the stress field near the crack tip leads one to define the mode mixity parameter as the ratio between shear σ_t and normal σ_n traction components at the interface at a given distance r from the crack tip along the interface corresponding to a reference length l (see Rice²⁶ and Hutchinson⁸): $\tan(\psi) = \left(\frac{\sigma_t}{\sigma_n}\right)_{r=l}$.

Most analyses of straight sided blister (SSB) delaminations from elastic substrates are based on the work described in Ref. 8, which gives a very elegant solution based on the plate post-buckling equilibrium for the delaminated part of the film (the Euler column) combined with a LEFM analysis of the interfacial crack using the Griffith criterion²⁷ to ascertain propagation (for $G(\psi) > G_c(\psi)$). The analytical Euler expression for the film deflection is given by⁸

$$w(y) = \frac{\delta}{2} \left(1 + \cos \frac{\pi}{b} y \right), \quad (2)$$

where δ is the amplitude of the blister and b is the blister half width. The mode mixity angle ψ at a reference distance $l = h$ from the crack front is given by⁸

$$\tan(\psi) = \frac{4 \cos \omega + \sqrt{3}(\delta/h) \sin \omega}{-4 \sin \omega + \sqrt{3}(\delta/h) \cos \omega}, \quad (3)$$

where the ω parameter depends on the elastic mismatch (i.e., on the Dundurs parameters, α and β) between the film and the substrate. In our study, $\beta = \alpha/4$ is used, which corresponds to the most common film/substrate system. Finally, the energy release rate G is^{8,15}

$$G = G_0 \left(1 - \frac{\sigma_c}{\sigma_0} \right) \left(1 + 3 \frac{\sigma_c}{\sigma_0} \right), \quad (4)$$

with $G_0 = h \frac{1-\nu_f}{E_f} \sigma_0^2$, which is the elastic energy per unit surface stored in the film and $\sigma_c = \frac{\pi^2}{12} \frac{E_f}{1-\nu_f^2} \left(\frac{h}{b}\right)^2$ is the critical buckling stress of the Euler column. It is important to note that G does not depend here on the elastic mismatch between the film and the substrate, as it is based on the equilibrium defined in Eq. (2). This latter expression is rigorously valid only in the case of an elastic film on an infinitely rigid substrate. As previously shown, in the case of a hard film on a soft substrate, a ‘‘Mexican hat’’ shape has to be taken into account. With our proposed model, we aim to investigate the robustness of the analytical approach developed by Hutchinson and Suo⁸ for cases of α approaching 1.

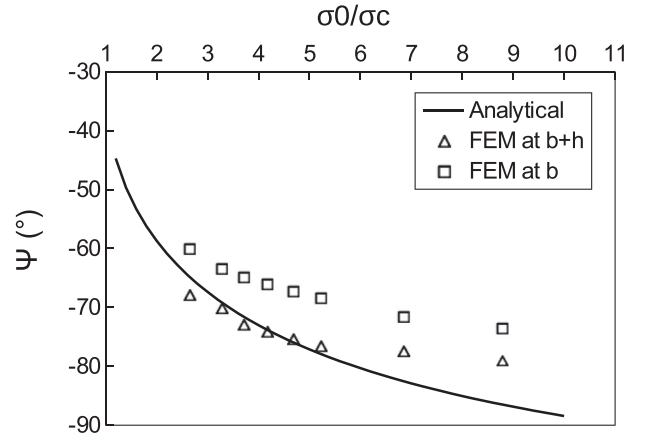


FIG. 3. Mode mixity ratio $\psi = f(\sigma_0/\sigma_c)$ for a hard substrate ($\alpha = -1$). Comparison between the analytical solution and FEM simulations.

First, we show how the two descriptions are equivalent in the case of an elastic film on an infinitely rigid substrate, despite the fundamental differences in approach discussed above. This is done by replacing the 3D substrate by an analytical rigid plane in the FEM model. The finite elements results and the analytical solutions are compared in Fig. 3, where the mode mixity parameter ψ is plotted versus the normalized applied stress σ_0/σ_c . It is shown that the FEM results at $(b+h)$ remarkably match the analytical behavior expected by LEFM⁸ in the case of a hard substrate, for $3 < \sigma_0/\sigma_c < 6$. This confirms the validity of our FE modeling. The main advance of the FEM simulation comes from the fact that there is no longer a mathematical singularity at the crack front so that ψ can now be accurately extracted at b , i.e., at the exact position of the crack. A similar behavior is observed, only shifted on lower values of $|\psi|$.

A parametric analysis was performed to obtain the evolution of the normalized energy release rate G/G_0 and the mode mixity ratio ψ as a function of the normalized stress σ_0/σ_c , for various α values (Figs. 4(a) and 4(b), respectively). The values of ψ are extracted from our calculations at the threshold of the fracture process zone ($x = b$).

It is observed in Fig. 4(a) that the numerical energy release rate stays roughly constant for low α values, in good agreement with the expected analytical solution given by Eq. (4). The implication is that the soft character of the substrate does not significantly affect the value of G for α ranging from -1 to approximately 0. Beyond this range, a significant increase in G is observed as already mentioned by Cotterell *et al.*²⁸ For example, an increase in G of approximately 68% for $\alpha = 0.82$ has been reported.

The analytical solutions predict that $|\psi|$ is quite similar, whatever the values of α (Fig. 4(b)). Such a behavior is also obtained from the numerical simulations for α ranging from -1 to 0.3. The difference between analytical and numerical solutions observed in Fig. 4(b) is ascribed to different data extraction methods described previously in Fig. 3. However, smaller values of $|\psi|$ are observed for $\alpha > 0.3$. These results are a direct assessment of the way the ‘‘Mexican hat’’ shape (accounted for in our calculations) influences the buckle propagation by modifying the loading applied at the interface. It is found that the ‘‘Mexican hat’’ shape decreases the mode II

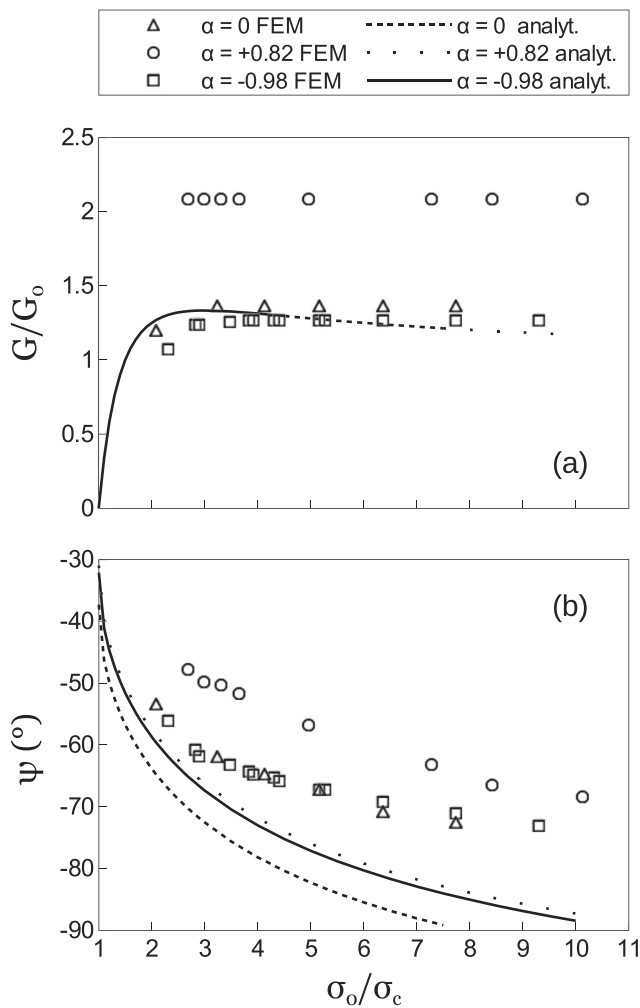


FIG. 4. Analytical solutions vs. FEM simulations for various α . (a) Energy release rate $G/G_0 = f(\sigma_0/\sigma_c)$. (b) Mode mixity ratio $\psi = f(\sigma_0/\sigma_c)$.

contribution (lower value of $|\psi|$), which leads to a lower effective interface toughness $G_c(\psi)$. At the same time, the energy release rate is much higher. Those two contributions strongly increase the effective driving force for fracture. This implies a more pronounced buckling structure, as the substrate becomes softer, even if the adhesion energy remains the same. For instance, for a given value of σ_0 , the final values of b are 2.2, 2.6, and $3.9 \mu\text{m}$ for values of α equal to -0.98 , 0 , and 0.82 , respectively. This supports the idea of a strong impact of a soft substrate on the buckle delamination and propagation behavior, as long as the linear elastic deformation hypothesis is valid for both the film and the substrate.

Finally, $|\psi|$ vs. α for a given stress is presented in Fig. 5, extracted from our FEM simulations. Two behaviors are highlighted: a constant regime for $|\psi|$ up to $\alpha = 0.3$ and then a continuous decrease. In Fig. 5, the numerical results strongly differ from the analytical ones, for which a parabolic dependence is expected.⁸ Indeed, in the constant regime, both t_n and t_t decrease in the same way. For α up to 0.3 , an increase in t_n and t_t is observed for increasing α , but the increase in t_n is greater than that of the t_t .

In conclusion, the “Mexican hat” morphology is characteristic of the elastic contrast between a film and its substrate. This specific shape of the delaminated region increases either the energy release rate (which was known²⁹) or the relative

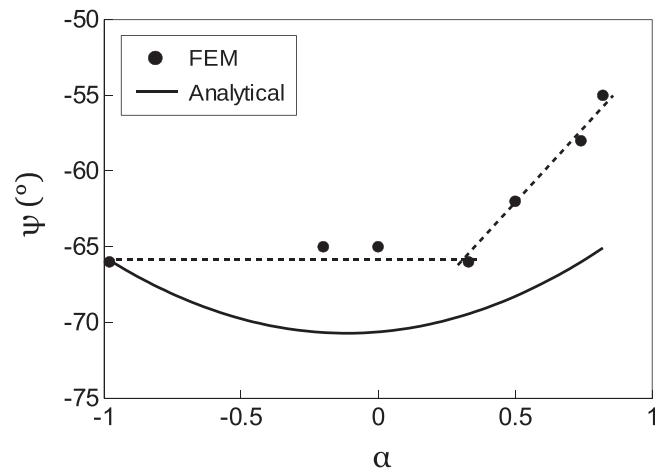


FIG. 5. ψ vs. α at a given stress ratio $\sigma_0/\sigma_c = 2.7$. Comparison between analytical solutions and FEM simulations for the case of $\beta = \alpha/4$.

proportion of mode I to mode II. These results advance the understanding of the mechanical behavior of a hard film on a soft substrate. Our findings provide updated insights into how the flexible devices (see, for instance, Kim *et al.*³⁰), which are promising revolutionary developments, can be damaged and how their life time can be modified.

This work was funded by the French National Research Agency program “CAPRICE” (ANR-14-CE07-0024-03), and it pertains to the French Government program “Investissements d’Avenir” (LABEX INTERACTIFS and ANR-11-LABX-0017-01).

¹E. A. Jagla, *Phys. Rev. B* **75**, 085405 (2007).

²M. J. Cordill, D. F. Bahr, N. R. Moody, and W. W. Gerberich, *Mater. Sci. Eng. A* **443**, 150–155 (2007).

³A. A. Abdallah, D. Kozodaev, P. C. P. Bouten, J. M. J. den Toonder, U. S. Schubert, and G. de With, *Thin Solid Films* **503**, 167–176 (2006).

⁴S.-J. Yu, X.-F. Xiao, M.-G. Chen, H. Zhou, J. Chen, P.-Z. Si, and Z.-W. Jiao, *Acta Mater.* **64**, 41–53 (2014).

⁵G. Parry, A. Cimetière, C. Coupeau, J. Colin, and J. Grilhé, *Phys. Rev. E* **74**(6), 066601 (2006).

⁶F. Foucher, A. Cimetière, C. Coupeau, J. Colin, and J. Grilhé, *Phys. Rev. Lett.* **97**, 096101 (2006).

⁷J. Colin, C. Coupeau, and J. Grilhé, *Phys. Rev. Lett.* **99**, 046101 (2007).

⁸J. W. Hutchinson and Z. Suo, *Adv. Appl. Mech.* **29**, 163–198 (1992).

⁹G. Parry, J. Colin, C. Coupeau, F. Foucher, A. Cimetière, and J. Grilhé, *Acta Mater.* **53**, 441–447 (2005).

¹⁰Y. Zhang and Y. Liu, *Acta Mech. Sinica* **30**, 927–932 (2014).

¹¹H. Mei, C. M. Landis, and R. Huang, *Mech. Mater.* **43**, 627–642 (2011).

¹²A. Lee, C. S. Litteken, R. H. Dauskardt, and W. D. Nix, *Acta Mater.* **53**, 609–616 (2005).

¹³J.-S. Wang and A. G. Evans, *Acta Mater.* **46**, 4993–5005 (1998).

¹⁴A. A. Volinsky, N. R. Moody, and W. W. Gerberich, *Acta Mater.* **50**, 441–466 (2002).

¹⁵M. W. Moon, H. M. Jensen, J. W. Hutchinson, K. H. Oh, and A. G. Evans, *J. Mech. Phys. Solids* **50**, 2355–2377 (2002).

¹⁶J.-Y. Faou, G. Parry, S. Grachev, and E. Barthel, *Phys. Rev. Lett.* **108**, 116102 (2012).

¹⁷F. Cleymand, C. Coupeau, and J. Grilhé, *Scripta Mater.* **44**, 2623–2627 (2001).

¹⁸A. A. Volinsky, N. R. Moody, M. L. Kottke, and W. W. Gerberich, *Philos. Mag. A* **82**, 3383–3391 (2002).

¹⁹V. Tvergaard and J. W. Hutchinson, *J. Mech. Phys. Solids* **40**(6), 1377–1397 (1992).

²⁰X. Xu and A. Needleman, *J. Mech. Phys. Solids* **42**(9), 1397–1434 (1994).

²¹F. Toth, F. G. Rammerstorfer, M. J. Cordill, and F. D. Fischer, *Acta Mater.* **61**, 2425–2433 (2013).

- ²²H. Sapardanis, V. Maurel, A. Köster, S. Duvinage, F. Borit, and V. Guipont, *Surf. Coat. Technol.* **291**, 430–443 (2016).
- ²³W. Zhu, L. Yang, J. W. Guo, Y. C. Zhou, and C. Lu, *Int. J. Plast.* **64**, 76–87 (2015).
- ²⁴J.-Y. Faou, G. Parry, S. Grachev, and E. Barthel, *J. Mech. Phys. Solids* **75**, 93–103 (2015).
- ²⁵K. M. Liechti and Y.-S. Chai, *J. Appl. Mech.* **58**, 680–687 (1991).
- ²⁶J. R. Rice, *J. Elasticity* **20**, 131–142 (1988).
- ²⁷A. A. Griffith, *Philos. Trans. R. Soc. London* **221**, 163–198 (1921).
- ²⁸B. Cotterell and Z. Chen, *Int. J. Fract.* **104**, 169–179 (2000).
- ²⁹H.-H. Yu and J. W. Hutchinson, *Int. J. Fract.* **113**, 39–55 (2002).
- ³⁰D.-H. Kim, N. Lu, Y. Huang, and J. A. Rogers, *Mater. Res. Soc. Bull.* **37**, 226–235 (2012).